Structural Engineering and Mechanics, *Vol. 62, No. 4 (2017) 417-430*
DOI: https://doi.org/10.12989/sem.2017.62.4.417

A review and analysis of circular UHPC filled steel tube columns under axial loading

An Le Hoang[*1, 2, 3] and Ekkehard Fehling[3a]

[1]*Division of Construction Computation, Institute for Computational Science, Ton Duc Thang University, Ho Chi Minh City, Vietnam*
[2]*Faculty of Civil Engineering, Ton Duc Thang University, Ho Chi Minh City, Vietnam*
[3]*Faculty of Civil and Environmental Engineering, Institute of Structural Engineering, University of Kassel, Kurt-Wolters-Strasse 3, 34125, Kassel, Germany*

(Received June 30, 2016, Revised October 17, 2016, Accepted December 22, 2016)

Abstract. Ultra high performance concrete (UHPC) has aroused interest around the world owing to superior mechanical and durability properties over conventional concrete. However, the application of UHPC in practice poses difficulties due to its inherent brittleness. UHPC filled in steel tube columns (UHPC-FSTCs) are capable of restricting the brittle failure of non-reinforced UHPC columns and forming a high performance member with enhancement of strength and ductility. Currently, research on UHPC-FSTCs remains very limited and there is relatively little information about the mechanical behavior of these columns. Therefore, this study presents a review of past experimental studies to have a deeper insight into the compressive behavior of UHPC-FSTCs under axial loading on entire section and on concrete core. Based on the test results obtained from Schneider (2006) and Xiong (2012), an analysis was conducted to investigate the influence of the confinement index (ξ) and diameter to steel tube thickness ratio (*D/t*) on the strength and the ductility in short circular UHPC-FSTCs. Furthermore, the appropriateness of current design codes including EC4, AISC, AIJ and previous analytical models for estimating the ultimate loads of composite columns was also examined by the comparison between the predictions and the test results. Finally, simplified formulae for predicting the ultimate loads in two types of loading pattern were proposed and verified.

Keywords: UHPC; confinement index; strength; ductility; steel tube columns; design codes

1. Introduction

Ultra high performance concrete (UHPC) is well known as a new cement-based material performing superior mechanical and durability properties over conventional concrete such as normal strength concrete (NSC) or high strength concrete (HSC). UHPC has a very high compressive strength exceeding of 150 MPa, possibly attaining 250 MPa and the addition of fibers reinforcement ensures the ductile behavior of UHPC under tension (AFGC 2002). Furthermore, it was also emphasized that depending on the composition and the temperature of heat - treatment process, the compressive strength of UHPC ranges between 200 MPa and 800 MPa (Richard and Cheyrezy 1995, Dugat *et al.* 1996). Schmidt and Fehling (2005) indicated that UHPC is characterized by a very dense matrix and a compressive strength ranging from 150 MPa to 200 MPa. Currently, there is no general definition for UHPC and it varies from country to country. It has been found in many previous experiments that, there is no difference in the compressive behavior between UHPC and ultra high strength concrete (UHSC), for example both UHPC and UHSC exhibit very high strength and secant modulus compared to NSC and HSC. However, it should be noted that UHSC and UHPC are not synonymous in some cases for the practical purpose. UHPC has its ingredients and mix proportions specifically prepared to generate particular properties for the expected use of the structure such as ultra high strength, better ductility, durability and lower permeability (Liew and Xiong 2015). In addition to the higher packing density of fines and compressive strength, which is defined for UHSC, the term ‘Ultra High Performance’ refers to the outstanding durability and low ratio water/cement (Schmidt and Fehling 2005).

The use of UHPC in construction has received significant recent research attention because of the excellent performance offered by UHPC over NSC and HSC. However, it can be argued that the inherently brittle nature of UHPC accompanying with very high strength causes a disadvantage of its applications in a large number of structures, especially the utilization of UHPC for seismically active regions (An *et al.* 2016). According to Empelmann *et al.* (2008), the possibility of the following methods should be considered to restrict the brittle failure of non-reinforced UHPC columns:

- Addition of the high strength steel fibres
- UHPC core confinement reinforcement by stirrups
- Using steel jacket pipe to provide confinement for UHPC core
- Using high-strength longitudinal reinforcement

∗Corresponding author, Ph.D. Student
E-mail: lehoangan@tdt.edu.vn
[a]Professor
E-mail: fehling@uni-kassel.de

http://www.techno-press.com/journals/sem&subpage=7 ISSN: 1225-4568 (Print), 1598-6217 (Online)

Likewise, Popa and Kiss (2013) reviewed some different methods of preventing UHPC column at brittle fracture and pointed out advantages as well as disadvantages of each method. The solutions in this study were shown as follows:

- Column wrapped with steel sheet.
- Composite column by combining UHPC core and NSC with reinforcement.
- Using steel stirrups to produce the confinement for UHPC.
- UHPC core wrapped by Fiber Reinforced Polymer (FRP).

Pu *et al.* (2004) stated that, for ultra high strength concrete (UHSC), if brittleness can not be overcome by itself, UHSC becomes a low performance concrete, thus leading to some limitations for its application in construction. From this point of view, these authors suggested that the effective way to improve the fragility performance of UHSC columns is using steel tubes, in which UHSC is filled. The combination of steel tube and UHSC results in the tremendous bearing capacity and excellent deformation.

Among the solutions mentioned above, the composite columns named as concrete filled steel tube columns (CFSTCs) have emerged as one of the dominant options for impeding the brittleness of UHPC or UHSC under compression (An and Fehling 2017a, b). To date, CFSTCs have found it way into a variety of structural applications such as multi-storey building, bridges and some supporting structures, particularly for earthquake resistance (Liew and Xiong 2012). This emanates from several advantages of CFSTCs in comparison with reinforced concrete or steel structures. For instance, due to continuous wrapping of concrete core by steel tube, CFSTCs perform higher stiffness, ductility, strength and better fireproofing property than reinforced concrete columns and steel columns (Morino *et al.* 2001). Moreover, the steel tube acts as a permanent formwork, which in turn reduces the cost on transportation and assemblage of columns (Han *et al.* 2014). The buckling deformation in the steel tube can be delayed by the concrete core owing to the confinement effect (Johansson 2002, Morino *et al.* 2001). The use of UHPC or UHSC for filling in steel tube columns is an attractive option, as this ensures that the reduction of column size and very high loading capacity can be achieved (Liew and Xiong 2010). A large number of experimental studies on the compressive behavior of CFTSCs have been undertaken, however the majority of previous experiments have mainly focused on NSC or HSC filled steel tube columns (NSC-FSTCs or HSC-FSTCs). Currently, research on the compressive behavior of UHPC or UHSC filled steel tube columns (UHPC-FSTCs or UHSC-FSTCs) remains very limited with only a handful of experimental studies reported (e.g., Liew and Xiong 2010, 2012, Liew *et al.* 2014, Xiong 2012, Tue *et al.* 2004a, b). Therefore, there is still a lack of information about the compressive behavior of CFSTCs using UHPC.

It is indicated that the international code for composite columns may be only suitable for normal strength concrete and steel (Liew *et al.* 2014, An and Fehling 2017b). The Eurocode 4 (EC4 2004) limits the concrete strengths class up to 60 N/mm^2, while the American Institute of Steel Construction (AISC 2005) only applies to CFST columns with normal weight concrete of strengths ranged between 21 MPa and 70 MPa. Additionally, the Chinese standard (DBJ 2003) and the Japanese code (AIJ 2001) limit the maximum compressive strength of concrete to 80 N/mm^2 and to 90 N/mm^2, respectively. With some recent advances, Australia standard (AS, 2014) for composite bridges and building allows the concrete cylinder compressive strengths up to 100 N/mm^2 (Aslani *et al.* 2015). Hence, to enable the application of UHPC in composite structures, the current design codes should be extended and updated by further experimental or theoretical research.

To address the aforementioned research gap, in this study, a comprehensive review on the compressive behavior of circular UHPC-FSTCs and UHSC-FSTCs through previous experimental studies and their applications was first presented and then followed by a discussion on the effect of the confinement index (ξ) and diameter to thickness ratio (D/t) on the strength and the ductility of short circular UHPC-FSTCs using cylinder compressive strengths of concrete higher than 150 MPa. Besides, the suitability of current design codes such as EC4, AISC, AIJ and some previous analytical models for confined concrete in circular CFSTCs was also validated by the comparison between predictions and test results obtained from Schneider (2006) and Xiong (2012). Finally, simplified formulae for predicting the ultimate loads of short circular UHPC-FSTCs under axial loading on entire section and on concrete core were proposed and verified.

2. Review of past experimental studies on UHPC-FSTCs and UHSC-FSTCs

As regards the classification of concrete compressive strength, the following limitations were suggested by Liew and Xiong (2012):

- Normal strength concrete (NSC): $f_c \leq 60$ MPa
- High strength concrete (HSC): $60 < f_c \leq 120$ MPa
- Ultra high strength concrete (UHSC): $f_c > 120$ MPa

where f_c is the compressive strength of concrete cylinder.

In terms of UHPC, the cylinder compressive strength were defined by many researchers with the values larger than 150 MPa (Fehling *et al.* 2014). Hence, in this context, the database of previous experimental tests on CFSTCs employing concrete with the cylinder compressive strengths higher than 120 MPa were collected and presented. Based on the compressive behavior of circular CFSTCs within the tests using various slenderness ratio, a short column is defined as length to diameter ratio $L/D \leq 4$, while a slender column is ranged with $L/D > 4$, where L is the effective length and D is the outer diameter of circular column (Kuranovas *et al.* 2009). However, Tao *et al.* (2013) recommended that L/D ratios should be ranged from 2 to 5 for short circular CFSTCs, thereby ignoring the effect of global imperfections. In this study, the short columns refer to $L/D \leq 4$ and slender columns refer to $L/D > 4$, this definition is also suggested by many previous researchers.

Kamo *et al.* (2015) introduced the application of using ultra high strength material to practical use for high-rise building in Japan. It was demonstrated that the combination between UHSC with compressive strength up to 160 MPa and ultra high strength steel tube (UHSS) with yield strength up to 780 MPa in CFSTCs ensures that the great reduction of both diameter and steel tube thickness is achieved in comparison with usual technique, resulting in a saving of amount of steel and concrete material. Furthermore, the increase of span in addition to high earthquake and fire resistance can be obtained by using these ultra high strength materials. Along with the presentation of Kamo *et al.* (2015), Matsumoto *et al.* (2015) reported the outline of the structural design of an ultra high-rise building using CFSTCs combining UHSS with yield strength of 780 MPa and UHPC core with compressive strength of 150 MPa. It was proven that the maximum axial load of these combine columns is 2.3 time as much as that of NSC-FSTCs. Due to the extremely large axial load capacity, the structural framing and architectural space can be achieved. They also concluded that by this combination, these members can have elastic deformation capability, which is suitable for satisfying high design criteria, especially for seismic design. A recommendation were given that in the future the application of UHPC to ultra high-rise building should be considered and expanded.

Blais and Couture (1999) reported the use of ultra high strength material for Sherbrooke pedestrian/bikeway bridge in Canada, which is the world's first major structure to be built with Reactive Powder Concrete (RPC). It is also well known that RPC is the most commonly available types of UHPC developed by French companies including Lafarge, Bouygues and Rhodia. It is indicated from this report that a significant increase of the compressive strength and ductility was achieved by the confinement of RPC core in a thin walled stainless steel tube. In the case of the Sherbrooke Footbridge, the compressive strength of RPC with fibres confined by steel tube and pre-stressed increases from 200 MPa to 350 MPa.

Pu *et al.* (2004) presented a series of experiments on 29 short circular UHSC-FSTCs under axial loading on entire section to investigate the efficiency of using various steel thicknesses in combination with UHSC. The test variables in this study consisted of steel tubes with the yield strengths between 313 MPa and 345 MPa, the thicknesses varied from 5 mm to 12.5 mm and outer diameters of 140 mm, and UHSC with cube compressive strengths between 156.7 MPa and 164.9 MPa. The experimental results revealed that short circular UHSC-FSTCs performed a very large displacement without disintegration and spalling. In addition, the residual load bearing capacity could be as high as 75.3%-135.2% of the peak strength but depending on the confinement index. It is supposed by these authors that UHSC-FSTCs can be applied in the construction of a kilometer high such as the super skyscraper, or arch ring of an arch bridge with no less than 1000 meters long span; for this reason, these columns were also defined as Kilometer-Compressible Material (KCM). Furthermore, with the use of UHSS, UHSC-FSTCs under compression do not undergo the sudden breakdown when approaching rupture, a large ductility is achieved with the start of plastic deformation of steel tube. Therefore, the authors asserted that UHSS should be considered for UHSC-FSTCs in order to solve the brittleness of UHSC completely. The equation for estimating the ultimate bearing capacity of short circular UHSC-FSTCs was also proposed in Pu *et al.* (2014) as follows

$$N_u = A_c \cdot f_c \cdot (1 + 1.2 \cdot \xi) \tag{1}$$

where N_u is the bearing capacity of UHSC-FSTCs; ξ is the confinement index and given by

$$\xi = \frac{A_s \cdot f_y}{A_c \cdot f_c} \tag{2}$$

where A_c and A_s are the cross section area of concrete core and steel tube in mm^2, respectively. f_y is the yield strength of steel tube in MPa, f_c is the cylinder compressive strength of UHSC in MPa.

Wang (2004) produced short circular CFSTCs using UHSC with compressive strength of 141 MPa and UHSS with yield stress up to 1026 MPa in order to show good prospects for the KCM in the building structure materials. The test variables in this study comprised different confinement indices and various steel tube diameters (D=118, 120, 122, 124, 126 mm) and steel thicknesses (t=3.5, 4.5, 5.5, 6.5, 7.5 mm). Test results of these columns showed that the increase in steel strength leads to not only higher ultimate bearing capacity but also the excellent deformability.

Guler *et al.* (2013) investigated on 12 short circular UHPC-FSTCs using UHPC with cylinder compressive strengths of 145 MPa and different steel thicknesses of 2.5, 3.0, 3.3, 3.65 mm tested under concentric loading on entire section. The EC4 design code was found to overestimate the axial bearing capacity of UHPC-FSTCs, while the American Concrete Institute (ACI) and AS, AIJ design codes were too conservative. These authors pointed out that due to little confinement effect induced by the steel tube to UHPC core during loading process up to peak load, the increase in steel thickness results in only the improvement of ductility after peak load and does not affect to the axial loading capacity. Based on the equations in ACI and AS, a modification for the equations of calculating axial bearing capacity were proposed with neglecting the confinement effect and given as follow

$$N_u = A_c \cdot f_c + A_s \cdot f_y \tag{3}$$

To investigate the influence of various types of concrete on the compressive behavior of slender circular CFSTCs and to establish the best option for practical design, Portolés *et al.* (2013) described 24 tests on slender circular tubular columns filled with NSC, HSC, UHSC for plain, bar reinforced and steel fiber reinforced columns. The test parameters included three eccentricities of loading (0, 20 and 50 mm), three types of concrete compressive strength (30, 90, 130 MPa), yield strengths of steel tube varied between 365.73 and 493.82 MPa. The use of HSC or UHSC infill was observed to be more effective with concentric loading than with eccentric loading. These authors stated that the steel fibers can substitute the steel reinforcement in the case of using lower strength of concrete (NSC), while the addition of steel fibers is not as useful in the case of using HSC or UHSC. Moreover, the improvement in ductility for slender columns is found to be easily achieved with small eccentricity but not with concrete strength or type of infill. These authors confirmed that although EC4 can be safely extended for slender circular HSC-FSTCs or UHSC-FSTCs under eccentric loading, it is less accurate for the prediction of columns under concentric loading.

A comprehensive research on circular CFSTCs with high strength materials has been presented by Liew and Xiong (2010, 2012), Liew *et al.* (2014) and Xiong (2012). In this study, UHSC with cylinder compressive strength up to 200 MPa and steel tube with yield strength up to 700 MPa were used. The behavior of short circular UHSC-FSTCs was examined under both axial loading on entire section and on concrete core. Based on the evaluation of test results, it was concluded that there is no significant development of confinement until the first peak load and a very small deformation achieved at the ultimate load; for this reason, the confinement effect should be neglected in short circular UHSC-FSTCs. With regard to loading pattern, these authors recommended that the columns should be loaded only on concrete core to obtain the maximum tri-axial confinement effect, thereby achieving the improved strength and ductility. For most of tests, due to the brittleness of UHSC core, a very loud cracking was heard around the first peak load, then following by a sudden drop in the load-shortening curves. After the load drop from the first peak load to the second peak load, a horizontal plateau was observed. The second peak load is herein defined as residual resistance. These researchers suggested that to satisfy the requirements of ductility, the residual resistance should be at least equal to 70% of the designed ultimate resistance. Although short circular UHSC-FSTCs can achieve the very high loading bearing capacities, the post peak behavior is still brittle, especially in the case of using lower values of the steel contribution ratio. The authors noted that to obtain sufficient ductility, a minimum of 1% volume of steel fibres should be added in UHSC mixture or the limitation on minimum steel contribution ratio as recommended in EC4 should be increased from 0.2 to 0.3. The EC4 code was found to underestimate the axial bearing capacities of short circular UHSC-FSTCs and could be safely extended for UHSC-FSTCs without consideration of confinement effect. It is suggested that the creep and shrinkage of UHSC should be further investigated for UHSC-FSTCs because they may affect to the bonding strength at the interface between the steel tube and the concrete core, which leads to the reduction in loading resistance.

The slender circular UHSC-FSTCs using high strength steel tube (HSS) subjected to concentric and eccentric loading was also tested by Xiong (2012). The test results revealed that the behavior of slender circular UHSC-FSTCs is ductile with gradual load reduction from the peak load without sudden failure. The author also noticed that the predictions from EC4 are quite conservative and the current scope of EC4 can be also safely extended for slender circular UHSC-FSTCs employing UHSC and HSS. Further, the combination of UHSC and HSS should be adopted for high-rise building and long-span structure due to the very high overall buckling compressive resistance and good ductility.

Yan and Feng (2008) carried out a series of tests on short circular UHPC-FSTCs using UHPC with volume of steel fibres up to 2% and the cube compressive strength up to 170 MPa. Based on the mechanical behavior of UHPC cylinders and UHPC-FSTCs under concentric loading on the entire section, the authors pointed out that the confinement effect on UHPC core is not as good as that on NSC core due to smaller lateral deformation of UHPC in the elastic stage. Thus, the interaction between UHPC and steel tube can be neglected in calculation of bearing capacity.

With the effort to compare the behavior of CFSTCs using various high performance concrete types, Chu (2014) has recently presented the tests on CFSTCs using UHSC with cylinder compressive strength up to 127 MPa under concentric loading on the entire section. The circular UHSC-FSTCs in this study included various slendernesses (L/D=3, 4, 9), steel tube thicknesses of 1.6, 3.2 and 4.8 mm and the outer diameter of 114 mm. The author reached the conclusion similarly to above mentions that UHPC exhibits less effective at enhancing axial strength of filled steel tube columns through confinement. Moreover, there were different failure mode of tested specimens, UHSC-FSTCs with slenderness ratio of 3 failed by radial expansion, while the columns with slenderness ratio of 4 and 9 failed by local buckling or shear. In addition to circular cross section, some specimens using rectangular or square shape were also tested to compare the effect of confinement in various cross sections.

With the current trend towards the use of UHPC-FSTCs in buildings and bridges, Tue *et al.* (2004b) proposed some application possibilities through experimental investigation of UHPC-FSTCs in the joints for tall building and truss bridges with the cylinder compressive strength of UHPC core between 150 MPa and 180 MPa. It was highlighted that the abrupt load drop of UHPC core can be overcome by sufficient confinement of steel tube under predominant compression load such as loading on only concrete core.

Schneider (2006) and Tue *et al.* (2004a) reported the extensive tests on short circular UHPC-FSTCs using steel tube thicknesses ranging from 1.5 mm to 8.0 mm under both loading on concrete core and entire section. In these tests, UHPC mixtures using coarse aggregate (Basalt Split) and having the cylinder compressive strengths of at least 150 MPa were chosen for filling in steel tube. Some other tests on short circular NSC-FSTCs and HSC-FSTCs were also carried out to provide a deeper insight into the difference among CFSTCs using various concrete strengths. The test results showed that NSC-FSTCs exhibit a remarkable ductile deformation capacity, while HSC-FSTCs perform a load drop continuously with increasing deformation after peak load. For UHPC-FSTCs, when loading on the entire section, the confinement effect is very small and both the steel tube and concrete section work separately until failure; however, the load imposing on concrete core leads to higher ultimate strength and better ductility compared to loading on entire section. The failure process of UHPC-FSTCs is characterized by the greater brittleness in post peak stage compared to NSC-FSTCs and HSC-FSTCs. These authors also maintained that the increase in steel tube thickness leads to the significant enhancement of post-peak behavior for UHPC-FSTCs. In addition to the strong autogenous shrinkage of UHPC core, the Poisson's ratio of UHPC core in elastic stage increases slightly (maximum value of Poisson's ratio of 0.32 at 70% of compressive strength), thus leading to an existing of a gap between concrete core and steel tube. As a result, UHPC-FSTCs need a higher stress level to excite a sufficient lateral strain to close this gap. The authors concluded that the influence of shrinkage should be considered in modelling and design of UHPC-FSTCs.

In brief, published research on the performance of UHPC-FSTCs and UHSC-FSTCs is still limited and there is a need for additional research data. As outlined above, except for the tests reported by Tue *et al.* (2004a), Schneider (2006), Liew and Xiong (2010, 2012), Liew *et al.* (2014) and Xiong (2012), most of experimental studies on these columns have mainly concerned with UHSC or UHPC having the cylinder compressive strengths lower than 150 MPa. Therefore, the behavior of CFSTCs using concrete with the cylinder compressive strengths higher than 150 MPa should be further investigated. It should be noted that, in this study, UHSC with the cylinder compressive strengths higher than 150 MPa can be named as UHPC due to the same compressive behavior.

3. Analysis of short circular UHPC-FSTCs under concentric loading

3.1 Discussion on the effect of key parameters on the strength and the ductility

There are some many variables that affect to the performance of circular CFSTCs such as concrete strength (f_c), steel yield strength (f_y), outer diameter (D), steel thickness (t), loading patterns, column length (L). Therefore, in this section, two key parameters including the ratio of diameter to steel thickness (D/t) and the confinement index ξ are selected to investigate their influences on the strength and the ductility. The basis confinement index ξ was used by different authors and defined as Eq. (2), this index reflects the combined influences of f_c, f_y, D, t. According to Han *et al.* (2005), Guler *et al.* (2013) and Portolés *et al.* (2013), for circular CFSTCs, some performance indices such as *CCR*, *SI* were defined to determine the degree of strength and ductility enhancement and they were given as follows:

- The level of strength enhancement can be represented by the concrete contribution ratio *CCR*, this index provides a quantitative measure of the benefit arising from concrete filling

$$CCR = \frac{N_{u,\,filled}}{N_{u,hollow}} \tag{4}$$

where $N_{u,\,filled}$ is the ultimate load of CFSTCs and $N_{u,\,hollow}$ is the ultimate load of corresponding unfilled hollow steel tube.

- The strength enhancement index *SI* may be introduced to the assess the load-carrying capacity of the composite section $N_{u,filled}$ relative to the sum of the strengths of the individual components and expressed

$$SI = \frac{N_{u,\,filled}}{A_s \cdot f_y + A_c \cdot f_c} \tag{5}$$

Larger values of *SI* reflect a positive interaction between the steel tube and concrete core, for example the concrete confinement and the delay of local buckling in the steel tube.

- The ductility of CFSTCs can be assessed in terms of the residual load (N_{res}) to ultimate load (N_u) ratio: N_{res}/N_u

In this study, the test results of short circular UHPC-FSTCs and UHSC-FSTCs reported by Schneider (2006) and Xiong (2012) with compressive strengths of concrete cylinders higher than 150 MPa were collected for calculating the key parameters and the performance indices. Tables 1 and 2 provide details of tested specimens in two groups including loading on concrete core and loading on entire section.

3.1.1 Concrete contribution ratio CCR

The relationships between *CCR* and ξ, *CCR* and *D/t* of short circular UHPC-FSTCs are plotted for the case of loading on entire section in Fig. 1. As can be seen, there is a substantial decrease in the *CCR* when the confinement index ξ is increased, while the *CCR* is drastically reduced with lower ratios of *D/t*. This observation may support to the fact that, for the columns having the same *D/t*, f_y and *L/D*, the increase in concrete strength leads to the reduction of the confinement index ξ, and the *CCR* consequently increases. In addition, it can be inferred that if the outer diameter is maintained but steel thickness is decreased, the *CCR* is increased due to higher *D/t* ratio. For instance, in Xiong's tests as shown in Table 2, in terms of the columns having the same f_c, f_y, D and L, when the confinement index ξ increases by around 2.1 times (from 0.304 to 0.649) and the steel thickness increases by 2 times (from 5 mm to 10 mm), the average decreases in the *CCR* are 47.8% and 58.6%, respectively. These results indicates that, for short circular UHPC-FSTCs under loading on entire section, the benefit of the concrete core is greater than that of the steel tube and much more critical with thinner steel tubes. The tendency of the *CCR* in this study is in agreement with the conclusions pointed out by Guler *et al.* (2013) and Portolés *et al.* (2013).

3.1.2 Strength index SI

The relationships between *SI* and ξ, *SI* and *D/t* of short circular UHPC-FSTCs under loading on entire section and on concrete core, were illustrated in Fig. 2 and Fig. 3, respectively. It was generally shown that, for both types of loading pattern, when the confinement index ξ increases or the ratio of *D/t* decreases, the *SI* increases. Nevertheless, it seems that the increase in the *SI* for the case of loading on

Table 1 Details of tested specimens under loading on concrete core

Ref.	No	ID	D (mm)	t (mm)	L (mm)	f_c (MPa)	f_y (MPa)	ξ	SI
Schneider (2006)	1	NB2.5	164.2	2.5	652	166.8	377	0.144	0.922
	2	NB3.0	189.0	3.0	756	166.8	398	0.159	0.952
	3	NB4.0	168.6	3.9	648	174.2	363	0.207	0.988
	4	NB4.8	169.0	4.8	645	176.7	399	0.280	0.960
	5	NB5.0	168.7	5.2	645	170.5	405	0.322	1.063
	6	NB5.6	168.8	5.7	650	173.4	452	0.391	1.051
	7	NB8.0	168.1	8.1	645	174.9	409	0.525	1.087
Xiong (2012)	1	S1-2-1(a)*	114.3	6.3	210	173.5	428	0.649	1.234

Table 2 Details of tested specimens under loading on entire section

Ref.	No	ID	D (mm)	t (mm)	L (mm)	f_c (MPa)	f_y (MPa)	ξ	CCR	SI
Schneider (2006)	1	NG1.5	186.1	1.5	735	155.7	371	0.079	--	0.860
	2	NG2.5	164.1	2.5	636	165.9	377	0.145	--	0.937
	3	NG3.0	189.2	3.0	730	173.1	398	0.153	--	0.894
	4	NG4.0	168.6	3.9	642	172.0	363	0.210	--	0.900
	5	NG4.8	169.0	4.8	643	176.2	399	0.281	--	0.966
	6	NG5.6	168.8	5.7	648	164.1	452	0.820	--	0.987
Xiong (2012)	1	S1-3-1(a)	114.3	3.6	250	173.5	403	0.323	4.984	1.172
	2	S1-3-1(b)	114.3	3.6	250	173.5	403	0.323	4.851	1.131
	3	S1-3-2(a)	114.3	3.6	250	184.2	403	0.304	5.138	1.154
	4	S1-3-2(b)	114.3	3.6	250	184.2	403	0.304	4.761	1.070
	5	S1-3-3(a)	114.3	6.3	250	173.5	428	0.649	2.512	1.124
	6	S1-3-3(b)	114.3	6.3	250	173.5	428	0.649	2.534	1.133
	7	S2-1-3	219.1	5.0	600	185.1	380	0.201	6.856	1.027
	8	S2-1-4	219.1	5.0	600	193.3	380	0.193	7.281	1.095
	9	S2-2-3	219.1	10.0	600	185.1	381	0.434	2.979	1.100
	10	S2-2-4	219.1	10.0	600	193.3	381	0.416	3.012	1.079
	11	S3-1-1	219.1	6.3	600	163.0	300	0.231	--	1.029
	12	S3-1-2	219.1	6.3	600	175.4	300	0.215	--	1.038
	13	S3-1-3	219.1	6.3	600	148.8	300	0.254	--	1.095
	14	S3-1-4	219.1	6.3	600	174.5	300	0.216	--	1.065

concrete core is higher than that of loading on the entire section. This is due to the load-carrying capacity of the composite section $N_{u,filled}$ increases quickly for the case of loading on concrete core and slowly for the case of loading on entire section with the increase in the confinement index ξ or with the reduction of D/t ratio. It is noticeable from Fig. 3 that the axial bearing capacities of UHPC-FSTCs under loading on the concrete core can be greater than the sum of the axial strengths of the concrete core and the steel tube individually when the confinement index ξ is higher than 0.3 or the D/t ratio is lower than 30. Thus, increasing the steel tube thickness or using higher steel yield strength in the case of loading on concrete core can provide better contribution towards the enhancement of the axial loading capacity compared to that in the case of loading on the entire section. This may be attributed to the fact that, for short circular UHPC-FSTCs, loading on concrete core results in higher confinement efficiency than loading on entire section (Liew and Xiong 2012, Xiong 2012).

3.1.3 The ratio of N_{res}/N_u

The relationships between the ratio of N_{res}/N_u and ξ, the ratio of N_{res}/N_u and D/t for both types of loading on entire section and on concrete core, were described in Fig. 4 and Fig. 5, respectively. It is apparent from these figures that the ratio of N_{res}/N_u is generally increased with the increasing the ξ and decreasing the ratio of D/t. Also, at the same values of confinement index ξ and the ratio of D/t, the case of loading on concrete core leads to the higher ratio of N_{res}/N_u compared to the case of loading on entire section. It is worth mentioning from the observation in Figs. 4-5 that, to ensure the ratio of N_{res}/N_u larger than 0.7 suggested by Liew *et al*. (2014) for the safe design, the values of the confinement index ξ should be higher than 0.3 or the values of the D/t ratio should be smaller than 30.

3.2 Comparison with design codes including EC4, AISC and AIJ

The axial bearing capacities of short circular UHPC-FSTCs obtained from Schneider (2006) and Xiong (2012) (N_{ue}) were compared with the predictions from design codes including EC4, AISC, and AIJ (N_{pre}). It is noted that the material partial safety factors were set to unity in all design calculations. The comparison results were presented in Table 3 for the type of loading on concrete core and in Table 4 for the type of loading on entire section.

With regard to short circular UHPC-FSTCs under loading on concrete core, it is revealed from the results in Table 3 that the ultimate loads predicted by EC4 were on average 4.5% greater than the test results, while the prediction from AISC and AIJ gave the ultimate loads about 14.2% and 7.5% lower than the test results, respectively. As a consequence, the prediction from AIJ is more conservative and safer than that from EC4 and AISC. Although EC4 code was capable of predicting the ultimate loads for short circular UHPC-FSTCs in two types of loading with a small difference in comparison with the test results, it still tended to overestimate. Overall, among these three codes, the proposed method by AISC is the best and safest predictor to estimate the ultimate loads of short circular UHPC-FSTCs under loading on entire section, while AIJ provision is the most reasonable and the most conservative to predict the ultimate loads of short circular UHPC-FSTCs under loading on concrete core.

The accuracy ratio is defined as the ratio between the ultimate load according to design code (N_{EC4}, N_{AISC}, N_{AIJ}) and the ultimate load obtained from the experimental test (N_{ue})

$$k_{EC4} = \frac{N_{EC4}}{N_{ue}} \tag{6}$$

$$k_{AISC} = \frac{N_{AISC}}{N_{ue}} \tag{7}$$

$$k_{AIJ} = \frac{N_{AIJ}}{N_{ue}} \tag{8}$$

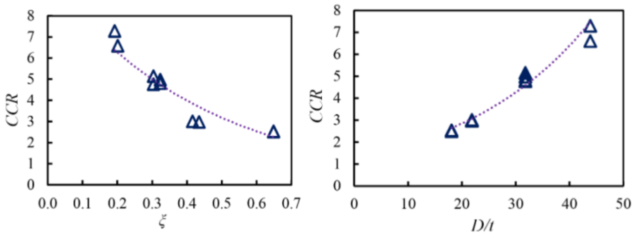

(a) (b)

Fig. 1 The relationships between *CCR* and ξ (a); *CCR* and *D/t* (b) for the columns under loading on entire section

To investigate the influence of the confinement index ξ and *D/t* ratio on the predictions of design codes, the dispersion plots for the accuracy ratios from EC4, AISC and AIJ against the confinement index ξ and the ratio of *D/t* are illustrated in Figs. 6-8. It is well established that the improvement in the ultimate load of short circular CFSTCs are mostly affected by the change in the confinement index ξ or the ratio of *D/t*. For instance, at high values of *D/t* ratio or at small values of confinement index ξ, there is obviously a reduction in confinement effect, thus leading to the decrease in the ultimate load. Fig. 6 indicates that for the

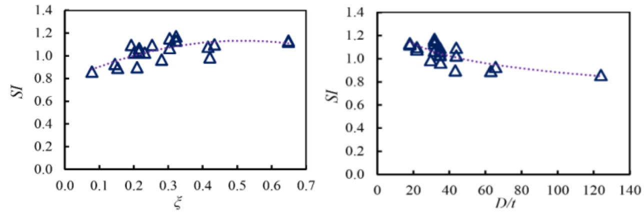

(a) (b)

Fig. 2 The relationships between *SI* and ξ (a); *SI* and *D/t* (b) for the columns under loading on entire section

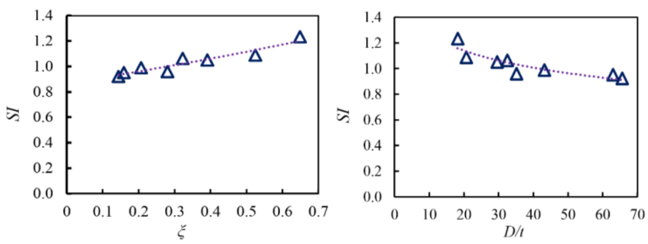

(a) (b)

Fig. 3 The relationships between *SI* and ξ (a); *SI* and *D/t* (b) for the columns under loading on concrete core

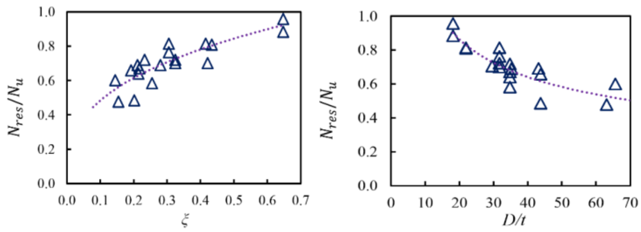

(a) (b)

Fig. 4 The relationships between N_{res}/N_u and ξ (a) and N_{res}/N_u and *D/t* (b) for the columns under loading on entire section

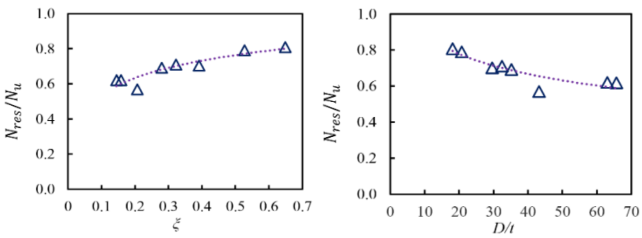

(a) (b)

Fig. 5 The relationships between N_{res}/N_u and ξ (a) and N_{res}/N_u and *D/t* (b) for the columns under loading on concrete core confinement index ξ higher than 0.3 and D/t ratio smaller than 30, EC4 provides very precise predictions. With the increase in D/t ratio or the decrease in the confinement index, the predicted ultimate load in EC4 is less accurate and tend to over-predict, while AISC provides safer estimation as depicted in Fig. 7. Among three codes, AISC can predict very well with higher D/t ratio and EC4 gives better predictions with higher confinement index ξ. Furthermore, the prediction from AIJ is more accurate for

Table 3 Comparisons between predicted ultimate loads and test results for the columns under loading on concrete core

Author	Specimen	N_{ue} (kN)	EC4 (2004) N_{pre} (kN)	EC4 (2004) N_{pre}/N_{ue}	AISC (2010) N_{pre} (kN)	AISC (2010) N_{pre}/N_{ue}	AIJ (2001) N_{pre} (kN)	AIJ (2001) N_{pre}/N_{ue}
Schneider (2006)	NB2.5	3501	3987.07	1.139	3136.58	0.896	3428.54	0.979
	NB3.0	4837	5343.97	1.105	4204.00	0.869	4612.86	0.954
	NB4.0	4216	4514.35	1.071	3695.79	0.877	3935.26	0.933
	NB4.8	4330	4792.18	1.107	3980.00	0.919	4249.79	0.981
	NB5.0	4751	4721.49	1.001	3944.65	0.837	4223.98	0.896
	NB5.6	4930	4977.72	1.010	4183.75	0.849	4542.19	0.921
	NB8.0	5254	5139.95	0.978	4414.52	0.840	4806.53	0.915
Xiong (2012)	S1-2-1(a)*	2866	2717.38	0.948	2226.55	0.777	2358.67	0.823
Mean value			1.045		0.858		0.925	
COV (Coefficient of Variation)			0.067		0.050		0.055	

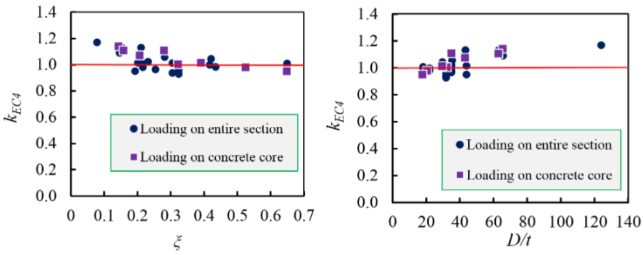

(a) (b)

Fig. 6 The relationships between k_{EC4} and ξ (a); k_{EC4} and D/t (b)

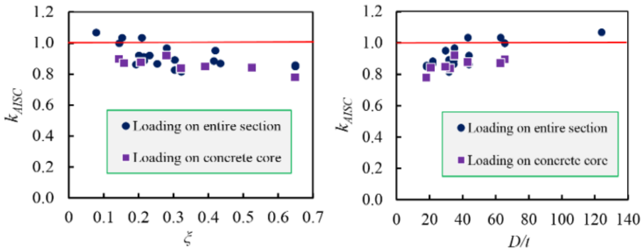

(a) (b)

Fig. 7 The relationships between k_{AISC} and ξ (a); k_{AISC} and D/t (b)

Table 4 Comparisons between predicted ultimate loads and test results for the columns under loading on entire section

Ref.	No	ID	N_{ue} (kN)	EC4 N_{pre}(kN)	EC4 N_{pre}/N_{ue}	AISC N_{pre}(kN)	AISC N_{pre}/N_{ue}	AIJ N_{pre}(kN)	AIJ N_{pre}/N_{ue}
Schneider (2006)	1	NG1.5	3800	4446.94	1.17	4057.92	1.07	4507.32	1.19
	2	NG2.5	3500	3820.68	1.09	3490.96	1.01	3903.90	1.12
	3	NG3.0	4700	5321.82	1.13	4861.49	1.03	5447.13	1.16
	4	NG4.0	3800	4301.02	1.13	3928.62	1.03	4420.98	1.16
	5	NG4.8	4350	4607.03	1.06	4202.10	0.97	4768.48	1.10
	6	NG5.6	4400	4600.87	1.05	4182.12	0.95	4814.65	1.09
Xiong (2012)	1	S1-3-1(a)	2422	2250.41	0.93	1971.51	0.81	2202.70	0.91
	2	S1-3-1(b)	2340	2250.41	0.96	1971.51	0.84	2202.70	0.94
	3	S1-3-2(a)	2497	2342.19	0.94	2061.45	0.83	2299.04	0.92
	4	S1-3-2(b)	2314	2342.19	1.01	2061.45	0.89	2299.04	0.99
	5	S1-3-3(a)	2610	2634.46	1.01	2235.83	0.86	2569.97	0.98
	6	S1-3-3(b)	2633	2634.46	1.00	2235.83	0.85	2569.97	0.98
	7	S2-1-3	7837	7967.04	1.02	7204.31	0.92	7975.27	1.02
	8	S2-1-4	8664	8238.03	0.95	7463.64	0.86	8256.72	0.95
	9	S2-2-3	9085	8930.20	0.98	7878.32	0.87	8936.91	0.98
	10	S2-2-4	9187	9173.63	1.00	8115.76	0.88	9192.08	1.00
	11	S3-1-1	6915	7083.31	1.02	6365.43	0.92	7060.15	1.02
	12	S3-1-2	7407	7471.08	1.01	6745.50	0.91	7475.23	1.01
	13	S3-1-3	6838	6606.08	0.97	5918.18	0.87	6584.82	0.96
	14	S3-1-4	7569	7436.50	0.98	6715.50	0.89	7445.10	0.98
Mean Value				1.021		0.912		1.024	
COV (Coefficient of Variation)				0.066		0.081		0.081	

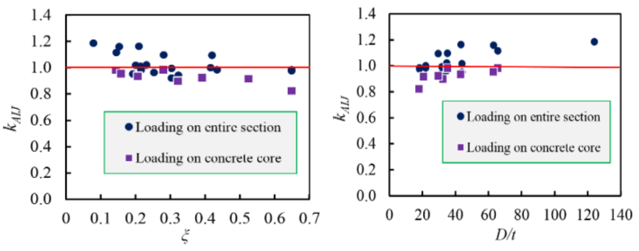

(a) (b)

Fig. 8 The relationships between k_{AIJ} and ξ (a); k_{AIJ} and D/t (b)

smaller D/t ratio and larger confinement index ξ. Fig. 8 shows that AIJ underestimates the ultimate loads for columns under loading on concrete core and it gives better prediction for confinement index lower than 0.3. However, for the columns under loading on entire section, AIJ overestimates the ultimate loads and it estimates accurately with the confinement index ξ higher than 0.3 or D/t ratio higher than 30.

3.3 Simplified formulae to predict the ultimate load

Back to the background of UHPC-FSTCs, it can be clearly seen that there are no empirical equations for predicting the ultimate load of this type of columns using the concrete with cylinder compressive strengths ranging from 150 MPa to 200 MPa. Some authors such as Guler *et al.* (2013), Yan and Feng (2008), Liew and Xiong (2010), Liew *et al.* (2014) assumed that the confinement effect should be ignored in the calculation of the ultimate loads, which means that the ultimate load is equal to the sum of ultimate strengths of concrete section and steel section individually. However, it can be observed in Pu *et al.* (2004) and Wang (2004) that the increase in the confinement index ξ or the decrease in D/t ratio may lead to the significant enhancement of the strength for short circular UHPC-FSTCs under loading on entire section. On the other hand, the confinement effect can be better generated in short circular UHPC-FSTCs under loading on concrete core, thereby resulting in higher ultimate loads compared to those in the case of loading on entire section (An and Fehling 2016, 2017a). Therefore, the confinement effect may be considered in calculation the ultimate load of short circular UHPC-FSTCs with wide range of steel thickness and the confinement index or with the type of loading on concrete core. It is expected that, by using the regression analysis from test results in Schneider (2006) and Xiong (2012), the simplified formulae for predicting the ultimate load can be proposed and separately established for each type of loading pattern.

3.3.1 Short circular UHPC-FSTCs under loading on entire section

A strength normalization parameter ψ was defined as

$$\psi = \frac{N_{ue} - N_c}{N_c} \tag{9}$$

where N_{ue} is the ultimate load measured in the test and N_c is the sectional capacity of concrete core and given by the following equation

$$N_c = A_c \cdot f_c \tag{10}$$

The plot of ψ with respect to the confinement index ξ based on the test results obtained from Schneider (2006) and Xiong (2012) is shown in Fig. 9(a). The regression coefficient R^2 has a value of 0.84, indicating a strong correlation between ψ and ξ. Hence, for short circular UHPC-FSTCs under loading on entire section, the ultimate load can be simply estimated by the equation as follow

$$N_u = (1 + 1.27 \cdot \xi) \cdot A_c \cdot f_c \tag{11}$$

3.3.2 Short circular UHPC-FSTCs under loading on concrete core

In the case of loading on concrete core, the ratio of f_{cc}/f_c between confined concrete compressive strength (f_{cc}) and unconfined concrete compressive strength (f_c) is plotted against the confinement index ξ in Fig. 9(b). The regression coefficient R^2 has a value of 1.00, showing a very strong correlation between f_{cc}/f_c and ξ. As a consequence, the formula for f_{cc} can be obtained by using the regression analysis, i.e.

$$f_{cc} = (0.8 + 1.8 \cdot \xi) \cdot f_c \tag{12}$$

Moreover, f_{cc} can be defined through the ratio of ultimate load to concrete cross-sectional area, which is given by the following equation

$$f_{cc} = \frac{N_u}{A_c} \tag{13}$$

Thus, the ultimate load of short circular UHPC-FSTCs under loading on concrete core can be easily determined by the following equation

$$N_u = (0.8 + 1.8 \cdot \xi) \cdot A_c \cdot f_c \tag{14}$$

It should be noted that the validity of Eq. (11) and Eq. (14) is: $150 \le f_c$ (MPa)≤ 200 and $235 \le f_y$ (MPa)≤ 460, $0.1 \le \xi \le 0.7$. Additional experimental research on short circular UHPC-FSTCs is much needed in the future to get more accurate predictions for the ultimate loads.

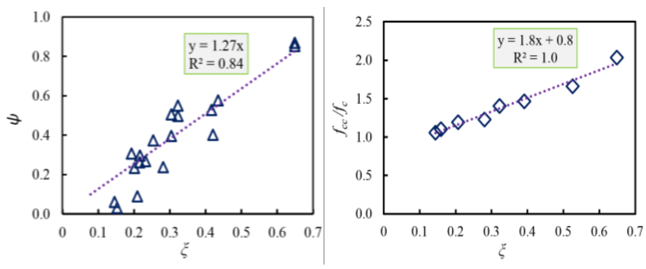

(a) (b)

Fig. 9 The relationship between ψ and ξ for the columns under loading on entire section (a) and the relationship between f_{cc}/f_c and ξ for the columns under loading on concrete core (b)

Table 5 The formulae for predicting the ultimate load in previous analytical models

Models	Expressions	Explanations
Susantha *et al.* (2001)	$v_c' = \frac{0.881}{10^6}\cdot\left(\frac{D}{t}\right)^3 - \frac{2.58}{10^4}\cdot\left(\frac{D}{t}\right)^2 + \frac{1.953}{10^2}\left(\frac{D}{t}\right) + 0.4011$ $v_c = 0.2312 + 0.3528\cdot v_c' - 0.1524\cdot\left(\frac{f_c}{f_y}\right) + 4.843\cdot v_c'\left(\frac{f_c}{f_y}\right) - 9.169\cdot\left(\frac{f_c}{f_y}\right)^2$ $\beta = v_c - v_s$ and $f_{rp} = \beta\cdot\frac{2\cdot t}{D-2\cdot t}\cdot f_y$ $f_{cc} = f_c + 4\cdot f_{rp}$ $N_u = A_c\cdot f_{cc} + A_s\cdot fy$	v_c : Poisson ratio of a steel tube filled with concrete v_s : Poisson ratio of a steel tube in yield condition, taken equal to 0.5 f_{rp} : Lateral pressure at the peak load f_{cc} : Confined compressive strength of the concrete N_u : Axial capacity of CFST column
Hatzigeorgiou (2008)	$\sigma_h = f_y\cdot\exp\left[\ln\left(\frac{D}{t}\right) + \ln(f_y) - 11\right]$ $f_{rp} = \frac{2\cdot t}{D-2\cdot t}\cdot\sigma_h$ and $f_{cc} = f_c + 4.3\cdot f_{rp}$ $f_{yc} = 0.5\cdot\left(\sigma_h - \sqrt{4\cdot f_y^2 - 3\cdot\sigma_h^2}\right)$; $N_u = A_c\cdot f_{cc} + A_s\cdot f_{yc}$	σ_h : Hoop stress of the steel f_{rp} : Mean confining stress f_{yc} : Compressive yield stress of steel tube
Johansson (2002)	$v_a = 0.3, v_c = 0.2, \varepsilon_v = 0.002$ $\varepsilon_{ahr} = \frac{\varepsilon_v(v_a - v_c)}{\left[1 + \frac{2\cdot t\cdot E_a}{(D-2\cdot t)\cdot E_c}\right]}$ and $\varepsilon_{ah} = -v_a\cdot\varepsilon_v + \varepsilon_{ahr}$ $\sigma_{ah} = \frac{E_a}{1-v_a^2}\cdot(\varepsilon_{ah} + v_a\cdot\varepsilon_{al})$; $\sigma_{al} = \frac{E_a}{1-v_a^2}\cdot(\varepsilon_v + v_a\cdot\varepsilon_{ah})$ $\sigma_{lat} = \sigma_{ah}\cdot\frac{2\cdot t}{D-2\cdot t}$ and $k = 1.25\cdot\left(1 + 0.062\cdot\frac{\sigma_{lat}}{f_{ct}}\right)\cdot f_c^{-0.21}$ $f_{cc} = f_c\cdot\left(\frac{\sigma_{lat}}{f_{ct}} + 1\right)^k$ and $N_u = A_c\cdot f_{cc} + A_s\cdot\sigma_{al}$	v_a, v_c, ε_v : Initial considered values ε_{ahr} : Restrained steel strain ε_{ah} : Final lateral strain of steel σ_{ah} : Steel's lateral stress σ_{al} : Steel's longitudinal stress σ_{lat} : Compressive confining pressure k : Parameter that reflects the effectiveness of confinement f_{ct} : Tensile strength of concrete
Sakino *et al.* (2004)	$\sigma_{ccB} = \gamma_u\cdot f_c + 4.1\cdot\sigma_r$ $\gamma_u = 1.67\cdot D_c^{-0.112}$ and $\sigma_r = \frac{-2\cdot t}{D-2\cdot t}\cdot\sigma_{s\theta}$ $\sigma_{s\theta} = \alpha_u\cdot\sigma_{sy}$ and $\sigma_{sz} = \beta_{uc}\cdot\sigma_{sy}$ $\alpha_u = -0.19; \beta_{uc} = 0.89$ $N_u = A_c\cdot\sigma_{ccB} + A_s\cdot\sigma_{sz}$	σ_{ccB} : Strength of confined concrete γ_u : Strength reduction factor for concrete and σ_r : Lateral pressure $\sigma_{s\theta}$: Hoop stress of steel tube in yield condition σ_{sy} : Tensile yield stress of steel σ_{sz} : Axial stress of steel tube in yield condition
Liang and Fragomeni (2009)	$f_{cc} = \gamma_c\cdot f_c + k_1\cdot f_{rp}$ $f_{rp} = \begin{cases} 0.7\cdot(v_e - v_s)\cdot\frac{2\cdot t}{D-2\cdot t}\cdot f_{sy}\ (\frac{D}{t}\le 47) \\ \left(0.006241 - 0.0000357\cdot\frac{D}{t}\right)\cdot f_{sy}\ (47\langle\frac{D}{t}\le 150) \end{cases}$ $v_e = 0.2312 + 0.3528\cdot v_e' - 0.1524\cdot\left(\frac{f_c}{f_{sy}}\right) + 4.843\cdot v_c'\left(\frac{f_c}{f_{sy}}\right) - 9.169\cdot\left(\frac{f_c}{f_{sy}}\right)^2$ $v_e' = \frac{0.881}{10^6}\cdot\left(\frac{D}{t}\right)^3 - \frac{2.58}{10^4}\cdot\left(\frac{D}{t}\right)^2 + \frac{1.953}{10^2}\left(\frac{D}{t}\right) + 0.4011$ $\gamma_c = 1.85\cdot D_c^{-0.135}(0.85\le\gamma_c\le 1)$; $\gamma_s = 1.458\cdot\left(\frac{D}{t}\right)^{-0.1}(0.9\le\gamma_s\le 1.1)$ $N_u = (\gamma_c\cdot f_c + 4.1\cdot f_{rp})\cdot A_c + \gamma_s\cdot f_{sy}\cdot A_s$	f_{cc} : Strength of confined concrete f_{rp} : Lateral pressure γ_c : Strength reduction factor for concrete γ_s : Strength factor for the steel tube f_{sy} : Tensile yield strength of steel v_e' : Empirical factor v_e : Poisson ratio of a steel tube filled with concrete

3.4 Comparison of ultimate loads between previous analytical models, proposed formulae and the test results

It has been found that there are various analytical models proposed by different researchers for evaluating the ultimate strength of circular CFST columns with taking into

Table 5 Continued

Models	Expressions	Explanations
Zhong and Miao (1988)	$p_o = -\frac{\alpha}{2}\cdot\frac{2\cdot\mu'+1}{\left[3\cdot\left(\mu'^2+\mu'+1\right)\right]^{1/2}}\cdot f_y$ $\mu' = -\frac{1}{2}-\frac{1}{2\cdot(\zeta+1)}$ $\zeta = \alpha\cdot\frac{f_y}{f_c};\alpha=\frac{A_s}{A_c}$ $N_u = N_c + N_s$ $N_s = \frac{\mu'+2}{\left[3\cdot\left(\mu'^2+\mu'+1\right)\right]^{1/2}}\cdot f_y\cdot A_s$ $N_c = (f_c + 4\cdot p_o)\cdot A_c$	p_o : Lateral confining pressure of the steel tube on the concrete N_c : Sectional strength of concrete core N_s : Sectional strength of steel tube
O'Shea and Bridge (2000)	$f_{cc} = f_c\cdot\left(-1.228+2.172\cdot\sqrt{1+\frac{7.46 f_l}{f_c}}-2\cdot\frac{p}{f_c}\right)\ (f_c \le 50MPa)$ $\frac{f_{cc}}{f_c} = \left(\frac{p}{f_t}+1\right)^k\ (80MPa \le f_c \le 100MPa)$ $p = p_{yield}\cdot\left(0.7-\sqrt{\frac{f_c}{f_y}}\right)\cdot\left(\frac{10}{3}\right)$ $p_{yield} = \frac{2\cdot f_y\cdot t}{D-2t}$ $k = 1.25\cdot\left(1+0.062\cdot\frac{p}{f_c}\right)\cdot(f_c)^{-0.21}$ $f_t = 0.558\sqrt{f_c}$ $N_u = A_c\cdot f_{cc} + A_s\cdot f_y$	f_{cc} : Compressive strength of confined concrete p : The applied confining pressure f_y : Yield strength of steel tube f_t : Tensile strength of concrete p_{yield} : The confining pressure in yield condition k : Parameter that reflects the effectiveness of confinement

account the confinement effect or not. Most of existing models have the approaches based on the confining theory and experiments, however these models have been mainly concerned with NSC or HSC confined by steel tube. It is likely that there is no suitable model for all concrete strengths, particularly for UHPC. Therefore, in this study, seven analytical models for the confined concrete in circular CFSTCs proposed by Susantha (2001), Hatzigeorgiou (2008), Johansson (2002), Sakino *et al.* (2004), Liang and Fragomeni (2009), Zhong and Miao (1988), O'Shea and Bridge (2000) were chosen to compute the ultimate loads of the tested columns in Tables 1 and 2. Table 5 shows expressions of seven analytical models for predicting the ultimate load of CFSTCs under compression. In addition to these models, the proposed equations in Guler *et al.* (2013), Liew and Xiong (2012) (Eq. (3)) and Pu *et al.* (2004) (Eq. (1)), which were the empirical formulae obtained from the own tests on short circular UHSC-FSTCs, were also used to calculate the ultimate loads for the columns under loading on the entire section. Then the predicted ultimate loads were compared against the measured results to verify the suitability of these proposed models. The ratios of the predicted ultimate loads to measured values (N_{pre}/N_{test}) versus the ratios of diameter to thickness (*D/t*) were plotted in Figs. 10-11 for the type of loading on entire section and in Fig. 12 for the type of loading on concrete core.

Analyzing the ratios of N_{pre}/N_{test} for short circular UHPC-FSTCs under loading on entire section in Fig. 10, only the model predicted by Sakino *et al.* (2004) gave the average ultimate load significantly higher than the test results with a difference of 15.5% and the COV of 15%, showing an unsatisfactory prediction. The models proposed by Susantha (2001), Johansson (2002) and Hatzigeorgiou (2008) overestimated the ultimate loads with differences of 10.6%, 6.9% and 3.4%, respectively, while the predictions of Liang and Fragomeni (2009), Zhong and Miao (1988), O'Shea and Bridge (2000), Guler *et al.* (2013), Liew and Xiong (2012) provided the safe sides with the average ultimate load slighly lower than the test results. However, except for the models of Johansson (2002), Pu *et al.* (2004) and this study, the values of COV of other models ranged from 9% to 15%, showing a large scatter in predictions. Observing the mean values and the COV in Fig. 11, the ratios of N_{pre}/N_{test} from the formulae proposed by Pu *et al.* (2004) and this study (Eq. (11)) were close to 1 and the standard deviations of the predictions were smaller than the other models with the corresponding COV of 7.8% and 7.4%. Among all models, the formulae proposed by Pu *et al.* (2004) (Eq. (1)) and this study (Eq. (11)) can reliably be used for computing the ultimate loads of short circular UHPC-FSTCs under loading on entire section.

In terms of short circular UHPC-FSTCs under loading on concrete core, in general, there was very little difference in the ultimate loads between the proposed models and the test results. The models of Susantha (2001), Johansson (2002), Hatzigeorgiou (2008) and O'Shea and Bridge (2000) gave the overestimations with the mean values ranged from 2.8% to 5.6% and the values of COV ranging between 5.5% and 9.1%, whereas the predictions from the models of Sakino *et al.* (2004), Liang and Fragomeni (2009) and Zhong and Miao (1988) were slighly lower than the experimental results with the mean values of 0.2%, 1.7% and 2.9%, respectively, and the corresponding COV of 5.8%, 6.6% and 9.7%, giving the safe sides. The model of Zhong and Miao (1988) presented larger variability in its individual predictions (COV=9.7%) compared to those of other models. In view of the aforementioned results, it appears that all models can reasonably to estimate the ultimate loads of short circular UHPC-FSTCs under loading on concrete core. However, among these models, the model proposed by Sakino *et al.* (2004) is the best predictor due to the safe prediction and the smallest difference of 0.2%, the COV of 0.055, compared to the test results. Furthermore, the ultimate loads predicted by Eq. (14) match the measured results very closely with the mean value of N_{pre}/N_{test} ratio of 1.008 and the COV of 0.035.

For the case of loading on entire section, the main reason for the overestimation and the large variability of the models proposed by Sakino *et al.* (2004), Susantha (2001), Johansson (2002) and Hatzigeorgiou (2008) in the calculation of the ultimate load may be attributed to the fact that the confinement effect provided by the steel tube in short circular UHPC-FSTCs is much lower than that in short circular NSC-FSTCs. These four models used the lateral confining pressure model based on NSC, thus

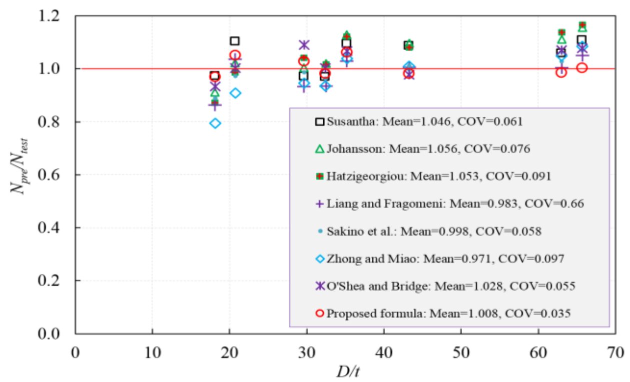

Fig. 12 The relationship between N_{pre}/N_{test} and D/t for the columns under loading on concrete core

generally overestimating the lateral confining pressure in terms of UHPC. However, the predicted ultimate loads in the models assumed by Liang and Fragomeni (2009), O'Shea and Bridge (2000) were conservative because these two models were developed for both NSC-FSTCs and HSC-FSTCs, in which the confining pressure was reduced using a reduction factor.

When all these models were applied for computing the ultimate load of short circular UHPC-FSTCs under loading on concrete section, the prediction was found to be more accurate. This can be explained by the fact that the confinement effect in this loading pattern is better than that in the case of loading on entire section, as has been proven in Schneider (2006) and Xiong (2012). In other words, the ultimate load when loading only on concrete core is increased by the lateral confining pressure of steel tube, which is obviously considered in all these models. On the other hand, the models of Sakino *et al.* (2004) and Liang and Fragomeni (2009) slightly underestimated due to the strength reduction factor reflecting some effects of the column size, the quality of concrete.

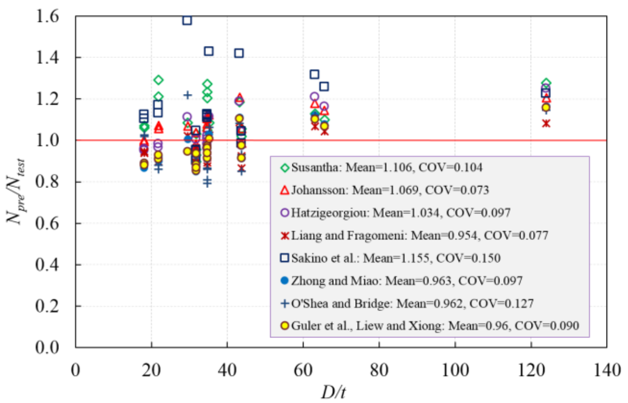

Fig. 10 The relationship between N_{pre}/N_{test} and D/t for the columns under loading on entire section

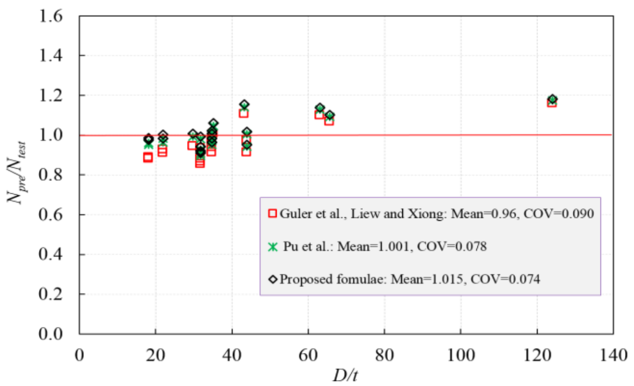

Fig. 11 The relationship between N_{pre}/N_{test} and D/t for the columns under loading on entire section (continued)

4. Conclusions

Based on the overview and the analysis in this study, some significant conclusions can be drawn as follows:

- The comprehensive review that was aimed at contributing significantly toward improving the understanding on the behavior of circular UHPC-FSTCs has been presented. In general, UHPC confined by steel tube is an appropriate solution to eliminate the risk of collapse of UHPC columns due to the brittle failure under high stress state. Furthermore, the circular UHPC-FSTCs under loading on entire section perform very weak confinement effect, which is caused by the small lateral deformation and the high shrinkage of UHPC core. However, the tri-axial confinement effect can be achieved and both the ductility and the strength of columns are improved if the load is applied to only concrete core.
- The *CCR* performance index that represents the benefit arising from the concrete filling into hollow steel tube is reduced with the increase in the confinement index ξ

and the decrease in D/t ratio. Thus, *CCR* is more significant for the thinner steel walls than for thicker ones.

• In terms of the strength index *SI*, higher confinement index ξ or smaller D/t ratio leads to the increase in *SI*, indicating a stronger interaction between UHPC core and steel tube. However, it is observed that the *SI* is higher than 1 if the confinement index is greater than 0.3 or ratio of D/t is smaller than 30. At the same parameters, the columns under loading on concrete core have better enhancement of the strength resistance and ductility compared to the columns under loading on entire section.

• To ensure the ratio of N_{res}/N_u larger than 0.7 suggested by Liew *et al.* (2014) for the safe design, the values of the confinement index ξ should be higher than 0.3 or the values of D/t ratio should be smaller than 30.

• The proposed method by AISC is a good and a safe predictor to estimate the ultimate loads of circular UHPC-FSTCs under loading on entire section, while AIJ provision is the most reliable to predict the ultimate loads of these columns under loading on concrete core owing to their conservativeness and good agreements compared to the test results.

• With the increase in D/t ratio or the decrease in the confinement index ξ, the predicted ultimate loads in EC4 and AIJ are less accurate, while AISC provides conservative estimation. Interestingly, AISC can predict very well with higher D/t ratio, while EC4 gives better predictions with higher confinement index.

• The simplified formulae are proposed for calculating the ultimate loads of short circular UHPC-FSTCs in two cases of loading pattern. The validity of two these formulae (Eq. 11 and Eq. 14) is $150 \le f_c$ (MPa) ≤ 200 and $235 \le f_y$ (MPa) ≤ 460, $0.1 \le \xi \le 0.7$. Except for the tests in Schneider (2006) and Xiong (2012), available database of these columns with compressive strengths of concrete cylinder higher than 150 MPa remain limited; thus it is not possible to verify the proposed formulae by the comparison with other test results in this paper. Nevertheless, these proposed formulae can be easily used by design engineers to estimate the ultimate loads.

• The previous analytical models of confined concrete in circular CFSTCs were used to calculate the ultimate loads of tested columns in Schneider (2006) and Xiong (2012). For the columns under loading on entire section, the formula proposed by Pu *et al.* (2004) is the best predictor. In the case of the columns under loading on concrete core, all analytical models are able to accurately predict the ultimate loads, but the model of Sakino *et al*. (2004) presents the best approach.

• Further research on UHPC-FSTCs is necessary to accelerate the use of UHPC in CFSTCs and to extend the design codes as well as the previous analytical models.

Acknowledgments

The work described in this paper was conducted by An Le Hoang as a part of his Doctoral study under the supervision of Prof. Dr.-Ing. Ekkehard Fehling. The first author would like to acknowledge the Vietnamese Government and Institute of Structural Engineering - University of Kassel and DAAD for the support of his full PhD scholarship.

References

An, L.H., Fehling, E. and Ismail M. (2016), "Numerical modelling of circular concrete filled steel tube stub columns", *Proceedings of HiperMat 2016 4th International Symposium on Ultra-High Performance Concrete and High Performance Construction Materials*, Kassel, Germany, March 9-11.

An, L.H. and Fehling, E. (2016), "Finite element analysis of circular steel tube confined UHPC stub columns", *Rilem Proceedings 105 of 1st International Conference on UHPC Materials and Structures (UHPC 2016-China)*, Changsha, China, October 27-30.

An, L.H. and Fehling, E. (2017a), "Numerical analysis of circular steel tube confined UHPC stub columns", *Comput. Concrete*, **19**(3), 263-273.

An, L.H. and Fehling, E. (2017b), "Analysis of circular steel tube confined UHPC stub columns", *Steel Compos. Struct*., **23**(6), 669-682.

American Concrete Institute (ACI) (2008), Building code requirements for structural concrete and commentary, *ACI 318-08*, Farmington Hills, MI, USA.

American Institute of Steel Construction (ANSI/AISC 360-10) (2010), Specification for Structural Steel Buildings, An American National Standard.

Architectural Institute of Japan (AIJ) (2001), Recommendation for design and construction of concrete filled steel tubular structures, Japan. (in Japanese)

Aslani, F., Uy, B., Tao, Z. and Mashiri, F. (2015), "Predicting the axial load capacity of high-strength concrete filled steel tubular columns", *Steel Compos. Struct.*, **19**(4), 967-993.

Association Française de Génie Civil (AFGC)/Service d'études techniques des routes et autoroutes (SETRA) (2002), Bétons fibrés à ultra-hautes performances, Recommandations provisoires, Janvier, France.

Blais, P.Y. and Couture, M. (1999), "Precast, prestressed pedestrian bridge: World's first reactive powder concrete structure", *PCI J.*, **44**(5), 60-71.

Chu, K. (2014), "Axial load behaviour of steel tube columns in-filled with various high-performance concretes", Master Thesis, Ryerson University, Toronto, Ontario.

DBJ 13-51-2003 (2003), Technical specification for concrete-filled steel tubular structures, China Planning Press, Beijing, China. (in Chinese)

Dugat, J., Roux, N. and Bernier, G. (1996), "Mechanical properties of reactive powder concrete", *Mater. Struct.*, **29**(4), 233-240.

Empelmann, M., Teutsch, M. and Steven, G. (2008) "Load-bearing behaviour of centrically loaded UHPFRC-columns", *Proceeding of Second International Symposium on Ultra High Performance Concrete*, Kassel, Germany.

Eurocode 4 (2004), Design of composite steel and concrete structures, Part 1.1, General rules and rules for Building, BS EN 1994-1-1, British Standards Institution, London, UK.

Fehling, E., Schmidt, M., Walraven, J., Leutbecher, T. and Fröhlich, S. (2014), *Ultra-High Performance Concrete: Fundamental - Design - Example*, Wilhelm Ernst & Sohn, Verlag für Architektur und technische Wissenschaften GmbH & Co. KG, Rotherstraße 21, 10245 Berlin, Germany.

Guler, S., Aydogan, M. and Copur, A. (2013), "Axial capacity and ductility of circular UHPC-filled steel tube columns", *Magazine Concrete Res.*, **65**(15), 898-905.

Han, L.H., Li, W. and Bjorhovde, R. (2014), "Development and advanced applications of concrete-filled steel tubular (CFST) structures: members", *J. Constr. Steel Res.*, **100**, 211-228.

Han, L.H., Yao, G.H., Chen, Z.P. and Yu, Q. (2005), "Experimental behavior of steel tube confined concrete (STCC) columns", *Steel Compos. Struct.*, **5**(6), 459-484.

Hatzigeorgiou, G.D. (2008), "Numerical model for the behavior and capacity of circular CFT columns, Part I: Theory", *Eng. Struct.*, **30**(6), 1573-1578.

Johansson, M. (2002), "The efficiency of passive confinement in CFT columns", *Steel Compos. Struct.*, **2**(5), 379-396.

Kamo, T., Ando, R., Sasaki, M., Suzuki, T. and Watanabe, Y. (2015), "Ultra high steel for sustainable building structure", Technical Report, Nippon Steel and Sumitomo Metal, No. 110, Japan.

Kuranovas, A., Goode, C.D Kvedaras, A.K. and Zhong, S. (2009), "Loading-bearing capacity of concrete-filled steel columns", *J. Civ. Eng. Manage.*, **15**(1), 21-33.

Liang, Q.Q. and Fragomeni, S. (2009), "Nonlinear analysis of circular concrete-filled steel tubular short columns under axial loading", *J. Constr. Steel Res.*, **65**(12), 2186-2196.

Liew, J.Y.R. and Xiong, D.X. (2010), "Experimental investigation on tubular columns infilled with ultra-high strength concrete", *Tubular Structures XIII*, The University of Hong Kong, 637-645.

Liew, J.Y.R. and Xiong, D.X. (2012), "Ultra-high strength concrete filled composite columns for multi-storey building construction", *Adv. Struct. Eng.*, **15**(9), 1487-1503.

Liew, J.Y.R., Xiong, M.X. and Xiong, D.X. (2014), "Design of high strength concrete filled tubular columns for tall buildings", *Int. J. High-Rise Build.*, **3**(3), 215-221.

Liew, J.Y.R. and Xiong , M.X. (2015), *Design Guide For Concrete Filled Tubular Members With High Strength Materials to Eurocode 4*, Research Publishing, Blk 12 Lorong Bakar Batu, 349568 Singapore.

Matsumoto, M.S., Komuro, K.T., Narihara, N.H., Kawamoto, K.S., Hosozawa, H.O. and Morita, M.K. (2012), "Structural design of an ultra-high rise building using concrete filled tubular column with ultra high strength materials", *Proceeding of 15th World Conference on Earthquake Engineering*, Lisbon, Portugal.

Morino, S., Uchikoshi, M. and Yamaguchi, I. (2001), "Concrete-filled steel tube column system - its advantages", *Steel Struct.*, **1**(1), 33-44.

O'Shea, M.D. and Bridge, R.Q (2000), "Design of circular thin-walled concrete filled steel tubes", *J. Struct. Eng.*, ASCE, **126**(11), 1295-1303.

Popa, M. and Kiss, Z. (2013), "State of the art regarding the protection of ultra-high performance concrete columns at brittle failure", *Proceeding of the 13th International Scientific Conference VSU'2013*, Sofia, Bulgaria.

Portolés, J.M., Serra, E. and Romero, M.L. (2013), "Influence of ultra-high strength infill in slender concrete-filled steel tubular columns", *J. Constr. Steel Res.*, **89**, 107-114.

Pu, X., Wan, C., Wang, Y., Pu, H. and Wang, C. (2004), "Kilometer compressible material and its preparation", *Proceeding of International Symposium on Ultra High Performance Concrete*, Kassel, Germany, March.

Richard, P. and Cheyrezy, M. (1995), "Composition of reactive powder concretes", *Cement Concrete Res.*, **25**(7), 1501-1511.

Sakino, K., Nakahara, H. Morino, S. and Nishiyama, I. (2004), "Behavior of centrally loaded concrete-filled steel-tube short columns", *J. Struct. Eng.*, ASCE, **130**(2), 180-188.

Schmidt, M. and Fehling, E. (2005), "Ultra-high-performance concrete: research, development and application in Europe", *ACI Struct. J., Special Publication*, **228**, 51-78.

Schneider, H. (2006), "Zum tragverhalten kurzer, umschnürter, kreisförmiger, druckglieder aus ungefasertem UHFB", Ph.D. Dissertation, University of Leipzig, Leipzig, Germany. (in German)

Standards Association of Australia (2014), AS/NZS 2327-2014, Composite structures, Sydney, Australia. (In preparation)

Susantha, K.A.S, Ge, H. and Usami, T. (2001), "Uniaxial stress-strain relationship of concrete confined by various shaped steel tubes", *Eng. Struct.*, **23**(10), 1331-1347.

Tao, Z., Wang, Z.B. and Yu, Q. (2013), "Finite element modelling of concrete filled steel stub columns under axial compression", *J. Constr. Steel Res.*, **89**, 121-131.

Tue, N.V., Schneider, H., Simsch, G. and Schmidt, D. (2004a), "Bearing capacity of stub columns made of NSC, HSC and UHPC confined by a steel tube", *Proceeding of International Symposium on Ultra High Performance Concrete*, Kassel, Germany, March.

Tue, N.V., Küchler, M., Schenck, G. and Jürgen, R. (2004b), "Application of UHPC filled tubes in buildings and bridges", *Proceeding of International Symposium on Ultra High Performance Concrete*, Kassel, Germany, March.

Wang, Y. (2004), "Research on preparation and mechanical performances of kilometer load-bearing material", Ph.D. Dissertation, Chongqing University, China. (in Chinese)

Xiong, D.X. (2012), "Structural behaviour of concrete filled steel tube with high strength materials", Ph.D. Dissertation, National University of Singapore, Singapore.

Yan, P.Y. and Feng, J.W. (2008), "Mechanical behavior of UHPC and UHPC filled steel tubular stub columns", *Proceeding of Second International Symposium on Ultra High Performance Concrete*, Kassel, Germany.

Zhong, S.T. and Miao, R.Y. (1988), "Stress-strain relationship and strength of concrete filled tubes", *Proceeding of Engineering Foundation Conference on Composite Constructions*, Henniker, New Hampshire, USA.

CC